Electromagnetic Form Factors of the Proton*

F. BUMILLER, M. CROISSIAUX,† E. DALLY,‡ AND R. HOFSTADTER
Department of Physics and High-Energy Physics Laboratory, Stanford University, Stanford, California
(Received July 20, 1961)

This paper reports experimental findings on the Dirac (F_1) and Pauli (F_2) form factors of the proton. The form factors have been obtained by using the Rosenbluth formula and the method of intersecting ellipses in analyzing the elastic electron-proton scattering cross sections. A range of energies covering the interval 200–1000 Mev for the incident electrons is explored. Scattering angles vary from 35° to 145°. Values as high as $q^2 \cong 31$ f^{-2} (q = energy-momentum transfer) are investigated, but form factors can be reliably determined only up to about $q^2 = 25$ f^{-2}. Splitting of the form factors is confirmed. The newly measured data are in good agreement with earlier Stanford data on the form factors and also with the predictions of a recent theoretical model of the proton. Consistency in determining the values of the form factors at different energies and angles gives support to the techniques of quantum electrodynamics up to $q^2 \cong 25$ f^{-2}. At the extreme conditions of this experiment (975 Mev, 145°) the behavior of the form factors may be exhibiting some anomaly.

I. INTRODUCTION

SINCE early 1955,[1] electron-scattering studies of the proton have been in progress at Stanford University when it was first shown that the proton is a structure more complicated than a point-charge and point-magnetic-moment. A summary of the findings on the proton made up to early 1960 was included in a recent book on electron-scattering tables.[2]

More recently an extension of the investigation to higher incident electron energies revealed important new features about the electromagnetic form factors of the proton which will now be sketched briefly in order to permit an understanding of the subject material of this paper.

The initial measurements[1,2] on the proton's Dirac (F_1) and Pauli (F_2) form factors showed that F_1 and F_2 were appreciably smaller than unity. This fact alone implied finite structure of the proton. The form factors (F_1,F_2) were found to lie in a region in which they were approximately equal to each other at energy-momentum transfers (q) less than $q^2 = 9.3$ f^{-2}. At this value of q^2 the measured ratio was $F_1/F_2 = 1.23 \pm 0.20$.[3] The value of this ratio was also in agreement with earlier measurements[4] of the quantity F_1/F_2. The early experiments were restricted to an angular range larger than 60° at the highest energies then available (~650 Mev) from the Stanford linear accelerator. They were also restricted because of the limitation imposed by the energy-handling ability of the 36-in. spectrometer used at that time. Under these conditions, the accuracy of the experiments did not allow a determination of F_1 and F_2 separately at $q^2 \gtrsim 9.3$ f^{-2}. Although the experiments cited[3,4] did indeed show that F_1 was slightly larger than F_2 at the same momentum transfer, the F_1/F_2 ratio was sufficiently close to unity so that for simplicity and for ease of calculation in most problems, the two form factors were usually taken to be equal to each other.

Recently the splitting of F_1 and F_2 was established at higher energies.[5–8] In the past year we have endeavored to increase the accuracy of our earlier results.[5–7] This paper reports the results of such an effort. We have also wished to compare our results with a theoretical model of the proton.[9] We shall see that the experimental proton results are in excellent agreement with that model.

II. EXPERIMENTAL METHOD

The basic idea of our method rests on a supposition which is in fact required by arguments of relativistic invariance, that each form factor is a function only of q^2. In this event one may solve for F_1 and F_2 by the "method of intersecting ellipses."[10,11]

In this method a measurement of a differential electron-proton scattering cross section at a given energy and angle (E_1, θ_1, respectively) determines, according to the Rosenbluth formula, Eq. (1), an ellipse in the F_1, F_2 plane. If a second measurement of a cross section

* This work was supported in part by the Office of Naval Research and the U. S. Atomic Energy Commission and by the U. S. Air Force, through the Office of Scientific Research of the Air Research and Development Command.

† Now at the Centre de Recherches Nucléaires, Strasbourg, France.

‡ Now at the Department of Physics, University of Zurich, Zurich, Switzerland.

[1] R. Hofstadter and R. W. McAllister, Phys. Rev. **98**, 217 (1955).

[2] R. Herman and R. Hofstadter, *High-Energy Electron-Scattering Tables* (Stanford University Press, Stanford, California, 1960).

[3] F. Bumiller and R. Hofstadter: See Fig. 8, p. 28, of reference 2.

[4] E. E. Chambers and R. Hofstadter, Phys. Rev. **103**, 1454 (1956).

[5] R. Hofstadter, F. Bumiller, and M. Croissiaux, *Proceedings of the 1960 Annual International Conference on High-Energy Physics at Rochester* (Interscience Publishers, Inc., New York, 1960), pp. 762–766.

[6] F. Bumiller, M. Croissiaux, and R. Hofstadter, Phys. Rev. Letters **5**, 261 (1960).

[7] R. Hofstadter, F. Bumiller, and M. Croissiaux, Phys. Rev. Letters **5**, 263 (1960).

[8] K. Berkelman, J. M. Cassels, D. N. Olson, and R. R. Wilson, *Proceedings of the 1960 Annual International Conference on High-Energy Physics at Rochester* (Interscience Publishers, Inc., New York, 1960), p. 757 ff. Cf. the account of this Rochester Conference paper subsequently published in Nature **188**, 94 (1960).

[9] R. Hofstadter and R. Herman, Phys. Rev. Letters **6**, 293 (1961).

[10] R. Hofstadter, *Ninth Annual International Conference on High-Energy Physics, Kiev, July, 1959 Plenary Session* IV, (Academy of Science, U.S.S.R., 1960), pp. 355-374.

[11] See reference 2, pp. 30–32 and Fig. 9.

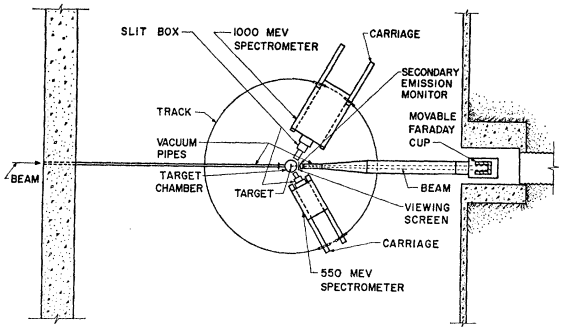

FIG. 1. This figure provides a schematic diagram of the experimental electron-scattering area, and shows the target chamber, the two spectrometers, the Faraday cup, the vacuum pipes, and other important parts of the apparatus. The track on which the spectrometers roll has an approximate radius of 13.5 ft.

is made at (E_2,θ_2) such that q^2 is the same as in the first measurement, a second ellipse can be determined. The requirement that the actual values of F_1 and F_2 be functions only of q^2 serves to determine the form factors at the point of intersection of the two ellipses. A third or fourth (etc.) measurement can also be used and if consistent determinations of F_1 and F_2 are obtained within experimental error, the Rosenbluth theory can be said to be confirmed and the values of F_1 and F_2 would be definitely established. Such consistency has been found in our measurements below $q^2 \lesssim 25$ f^{-2}, but a determination of F_1 and F_2 at our very highest values of q^2 ($\cong$30 f^{-2}) needs further discussion.

Two ellipses will intersect in four points in the F_1, F_2 plane. It is easy to see that the normalization of the electric charge and the static magnetic moment of the proton serve to define only the set in the first quadrant with values: $F_1(0)=+1.0$; $F_2(0)=+1.0$.

In the above manner we employ the following formulas:

$$\frac{d\sigma}{d\Omega}=\sigma_{NS}\left\{F_1^2(q^2)+\frac{\hbar^2q^2}{4M^2c^2}\left[2\{F_1(q^2)+KF_2(q^2)\}^2\times\tan^2\frac{\theta}{2}+K^2F_2^2(q^2)\right]\right\}, \quad (1)$$

where

$$\sigma_{NS}=\left(\frac{e^2}{2E}\right)^2\frac{\cos^2(\theta/2)}{\sin^4(\theta/2)}\frac{1}{[1+(2E/Mc^2)\sin^2(\theta/2)]}, \quad (2)$$

and

$$q=\frac{(2E/\hbar c)\sin(\theta/2)}{[1+(2E/Mc^2)\sin^2(\theta/2)]^{\frac{1}{2}}}, \quad (3)$$

where the symbols have their usual significance and K has the numerical value of 1.79.

We may then write

$$d\sigma/d\Omega=\sigma_{NS}[a_{11}F_1^2+a_{12}F_1F_2+a_{22}F_2^2], \quad (4)$$

where

$$a_{11}=1+(\hbar^2q^2/2M^2c^2)\tan^2(\theta/2), \quad (5)$$

$$a_{12}=(\hbar^2q^2K/M^2c^2)\tan^2(\theta/2), \quad (6)$$

$$a_{22}=(\hbar^2q^2K^2/2M^2c^2)[\tan^2(\theta/2)+\tfrac{1}{2}]. \quad (7)$$

Values of σ_{NS}, a_{11}, a_{12}, and a_{22} may be found from the tables of reference 2 and the ellipses can be plotted according to Eq. (4). It is thus necessary to find the experimental values of the cross section $d\sigma/d\Omega$ at many settings of energy E and scattering angle θ.

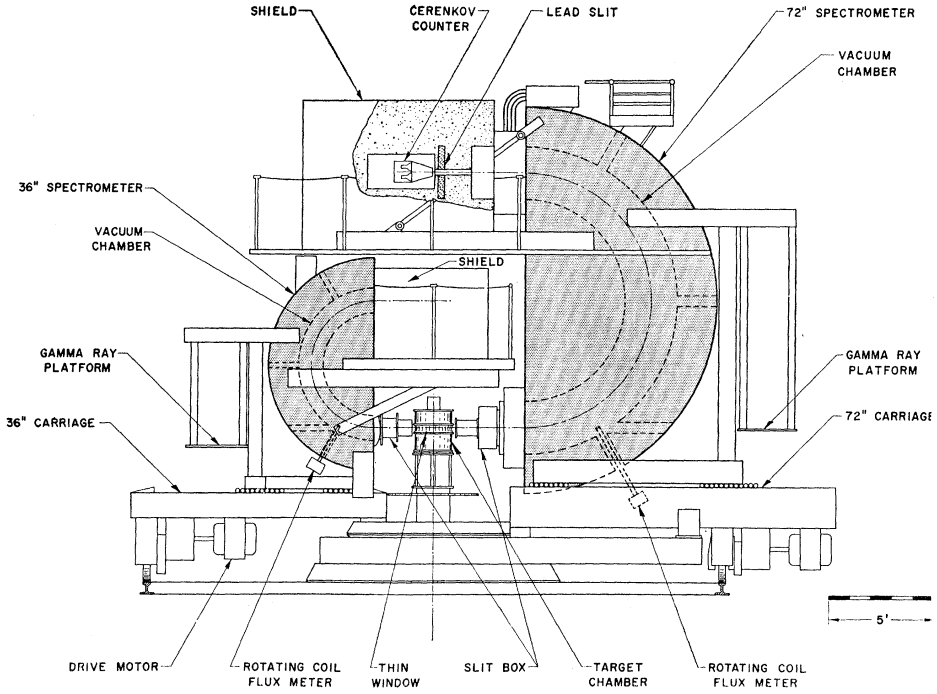

FIG. 2. This figure shows a side view of the spectrometers, target assembly, counters and shields, and other parts of the apparatus. The weight of the 72-in. spectrometer and the massive counter shield is in the neighborhood of 200 tons. The pulsed nature of the beam of the linear accelerator makes it necessary to use such a massive shield.

III. MEASUREMENTS OF ELASTIC CROSS SECTIONS

Most of the cross sections reported in this paper are entirely new and have been determined over a period of the last year. Some of the cross sections were recalculated from older published work[3,5,6] using new and better determinations of spectrometer characteristics and also new values of the radiative corrections.

All measurements given in this paper are absolute cross sections and were measured with the apparatus described in references 5–7 and also more thoroughly in reference 12. Figures 1 and 2 provide, respectively, schematic drawings of the experimental area and the double spectrometer system. The rotating coil flux meters, which are very important components of the two spectrometers, have been described briefly[13] and will be discussed subsequently in more detail.[14]

With such apparatus, which includes a Faraday cup for absolute normalization of the incident electron beam, we have taken 150 elastic scattering curves of appearance comparable with those shown in Figs. 3 and 4. The two elastic peaks chosen in Figs. 3 and 4 illustrate the quality of the small-angle and large-angle determinations. It is to be noted that the target material was polyethylene (CH_2). The carbon backgrounds were taken separately using graphite targets. The carbon background points have been fitted by least-squares analyses of the data.

In obtaining absolute data, various quantities and properties of the apparatus have to be determined with fair precision. For example, the momentum calibration of the magnetic spectrometer must be known, as well as the dispersion (number of inches per percent spread of momentum) at the exit slit of the spectrometer. Slit openings, target thickness, target density, etc., must all be determined with accuracy. A moving polyethylene target was used to prevent depletion of the hydrogen content through bombardment and heating of the target. It must also be known that the Faraday cup does not miss some of the beam which spreads after leaving the target. "Thick" target effects must be avoided in order to insure good geometry of the rays entering the spectrometer. One must also be sure that the entrance slits that are used are not too large so that parts of the electron trajectories do not hit the walls of the spectrometer or pass through a region in which the magnetic focusing properties are unsatisfactory.

The electron trajectories in the spectrometer were studied ("optics" study) by placing a fluorescent screen in the focal region of the spectrometer and viewing the

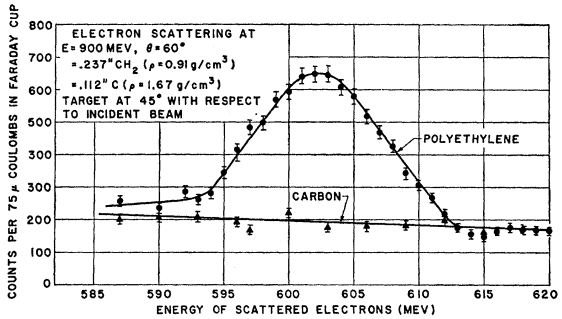

FIG. 3. An electron scattering peak observed at 60° from a polyethylene target at an incident energy of 900 Mev. This curve was taken with the 72-in. spectrometer and illustrates the quality of runs taken at the small angles. The value of the abscissa gives the directly-measured energy of the scattered electrons. The ordinate is proportional to the differential cross section in cm²/sr Mev.

screen remotely with a television system. For this purpose the linear accelerator beam was led directly into the spectrometer, which was set at the zero degree setting of the scattering angle. A small deflecting magnet placed in front of the spectrometer bent the beam up down to simulate the entrance conditions of scattered electrons. The spectrometer scattering angle was varied slightly from zero to take care of the horizontal dimension. In the optics study, the angle of inclination of the focal plane, the movement of the focus with target position, the depth of focus, the energy calibration, the dispersion, etc., were investigated in detail.

It is further necessary to know the efficiency of the Čerenkov detector in order to be certain that any loss in this counter is recognized and allowed for. The Čerenkov counter efficiency was investigated with the help of a multi-channel analyzer and its pulse distributions examined during almost every run, and we believe the efficiency is so close to 100% that we have arbitrarily taken 100% as its efficiency. A Lucite Čerenkov counter and two different liquid Čerenkov counters were used in the efficiency studies and in the measurements and no discrepancies among the counters were

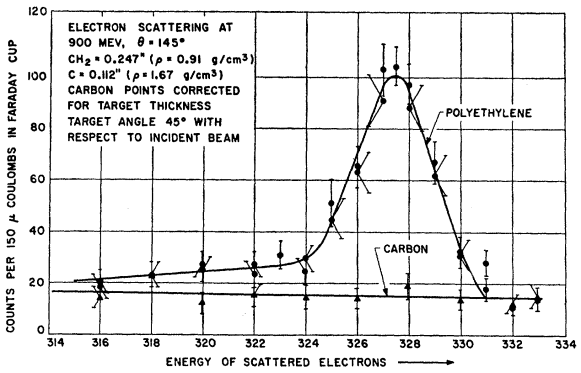

FIG. 4. This figure is similar to Fig. 3 but shows the quality of peaks taken at large angles, in this case, 145° at an incident energy of 900 Mev.

[12] R. Hofstadter, F. Bumiller, B. R. Chambers, and M. Croissiaux, *Proceedings of an International Conference on Instrumentation for High-Energy Physics* (Interscience Publishers, Inc., New York, 1961) pp. 310–315.

[13] F. Bumiller, J. F. Oeser, and E. B. Dally, *Proceedings of an International Conference on Instrumentation for High-Energy Physics* (Interscience Publishers, Inc., New York, 1961) pp. 308–309.

[14] F. Bumiller and J. F. Oeser (to be published).

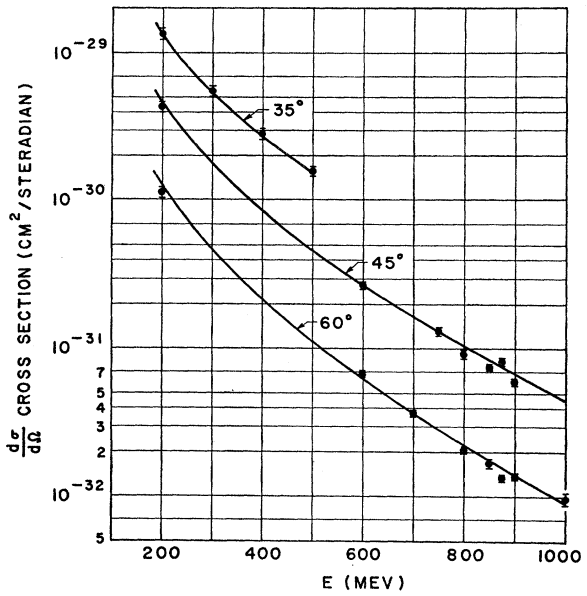

FIG. 5. The elastic electron-proton scattering cross sections in the range 35° to 60°. The experimental points are shown with appropriate error bars and correspond to the values in the sixth column of Table I. The solid line refers to the calculated cross sections (last column of Table I) using the form factors found in these experiments.

noted. All the above matters, and others not mentioned, have been studied in detail too great to be reproduced here. Various errors introduced at all stages in the measurements have been investigated and, e.g., such matters as the widths at half-maximum of the experimental peaks are thought to be understood. As a result of such considerations we present in the Appendix a discussion of some of their actual numerical values.

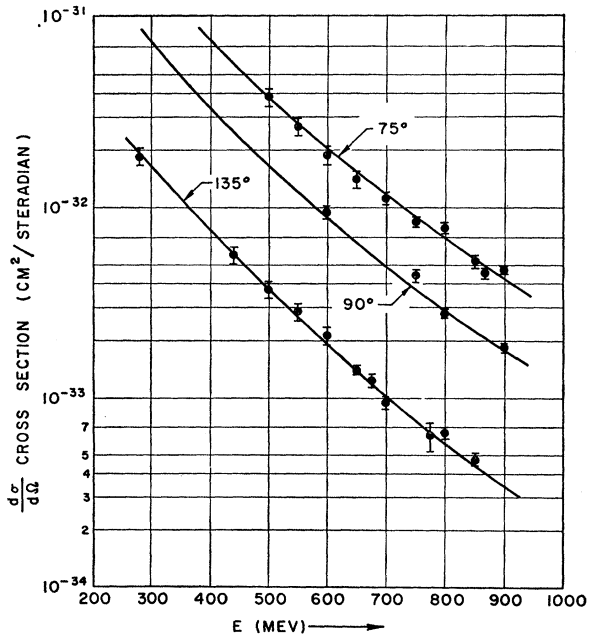

FIG. 6. This figure is similar to Fig. 5 and corresponds to the angular range 75° to 135°.

Since the elastic peaks are measured usually over a range extending only to energies 5% or less below the value at the peak, it is necessary to make radiative corrections for the area under the tail of the curve which is not examined. Such radiative corrections have been applied regularly in the past. Recently, an improved calculation has been made by Sobottka[15,16] which allows for the recoil of the struck proton. An even more accurate calculation has been carried out by Tsai.[17] Since the two calculations agree quite closely, we have chosen the simpler Sobottka correction to use with our data. Typical values of the radiative corrections including straggling are 30% at large angles (~135°) for a "ΔE" interval equal to the half-width and 25% at a small angle (~60°). We have usually used values of ΔE equal to the half-widths, since the polyethylene-carbon subtraction procedure involves a relatively large error in the tails of the proton curves beyond a few percent below the peak. The radiative corrections are, however, not sensitive to either angle or energy. As will be shown below, this implies that only very small errors in F_1 and F_2 can result from possible larger errors in the values of the radiative corrections. Thus the choice between the Sobottka calculation or the Tsai calculation has negligible influence on the form factors. This is also true whether one uses ΔE intervals of 1% or 5% consistently.

When the radiative corrections as well as other known corrections are applied to the data, we obtain the final results for the experimentally measured elastic cross sections shown in Table I. The results given in Table I are also shown in Figs. 5, 6, and 7 and appropriate error bars are attached to each experimental point. Although 150 individual peaks were measured, a number of determinations at the same energy and angle have been combined together to give a weighted mean cross section. Therefore Figs. 5, 6, and 7 show only 58 measured points.

A comparison of these results with those given in references 5, 6, and 7 shows that the earlier results were correct within experimental errors quoted in those references. However, certain small systematic differences can be observed: The newer small-angle measurements are generally a bit lower than the older ones. This is a direct consequence of new and improved knowledge of the energy calibration and dispersion properties of the 72-in. spectrometer. The new large-angle measurements are generally in good agreement with the older measurements but a little higher on the average.

We wish to call particular attention to the high-energy results at 145° shown in Fig. 7. The cross sec-

[15] S. Sobottka, Phys. Rev. **118**, 831 (1960).
[16] S. Sobottka, thesis, Stanford University, 1960 (unpublished).
[17] Y.-S. Tsai, Phys. Rev. **122**, 1898 (1961). Note that straggling corrections are not calculated in this paper.

TABLE I. Experimental elastic cross sections and other pertinent data.

E (Mev)	θ (degree)	q^2 (f^{-2})	% radiative correction	%ΔE used in rad. corr.	$(d\sigma/d\Omega)_{\text{exp}}$ (10^{-32} cm^2/sr)	Possible error	Possible error in %	$(d\sigma/d\Omega)_{\text{calc}}$[a] ($10^{-32}$ cm^2/sr)
200	35	0.358	15.0	4.5	1340	110	8.2	1330
	45	0.566	15.0	4.5	430	35	8.2	452
	60	0.928	16.0	4.5	113	9	8.0	126
280	135	4.42	17.0	4.5	1.86	0.18	9.7	1.88
300	35	0.790	16.0	4.5	550	44	8.0	538
400	35	1.38	16.0	4.5	281	23	8.2	271
440	135	9.38	18.0	4.5	0.565	0.056	10.0	0.585
500	35	2.12	17.0	4.5	156	12	7.7	153
	75	6.82	18.0	4.5	3.80	0.38	10.0	3.79
	135	11.48	17.0	4.5	0.370	0.037	10.0	0.380
550	75	8.03	18.0	4.5	2.65	0.26	10.0	2.76
	135	13.26	17.0	4.5	0.285	0.029	10.0	0.270
600	45	4.56	27.6	1.46	26.5	1.4	5.3	26.4
	60	7.00	25.9	1.87	6.70	0.41	6.1	6.19
	75	9.30	16.0	4.5	1.88	0.19	10.0	2.06
	90	11.28	28.9	1.57	0.944	0.071	7.5	0.878
	135	15.09	30.5	1.12	0.212	0.023	10.8	0.188
	145	15.55	30.3	1.09	0.141	0.022	15.6	0.155
650	75	10.63	19.0	4.5	1.40	0.14	10.0	1.56
	135	16.97	29.3	1.34	0.140	0.007	5.0	0.138
675	135	17.93	30.6	1.22	0.123	0.009	7.3	0.120
700	60	9.17	27.5	1.76	3.62	0.16	4.4	3.63
	75	12.01	25.8	2.01	1.12	0.074	6.6	1.18
	135	18.9	30.3	1.23	0.940	0.072	7.6	0.102
	145	19.42	29.0	1.35	0.0747	0.0032	4.3	0.0851
750	45	6.86	25.6	1.94	13.0	0.92	7.1	13.2
	75	13.45	26.3	1.93	0.839	0.049	5.8	0.910
	90	16.06	26.1	2.15	0.439	0.034	7.7	0.368
	145	21.42	30.4	1.15	0.0643	0.0039	6.1	0.0650
775	135	21.83	30.6	1.19	0.0630	0.0109	17.3	0.0675
	145	22.42	31.3	1.06	0.0616	0.0069	11.2	0.0560
800	45	7.70	25.4	2.12	9.12	0.65	7.1	10.3
	60	11.52	25.5	2.08	2.07	0.08	3.9	2.24
	75	14.93	23.8	2.37	0.782	0.052	6.6	0.684
	90	17.74	27.0	1.91	0.277	0.012	4.3	0.287
	135	22.85	27.6	1.51	0.0655	0.0043	6.6	0.0593
	145	23.44	30.2	1.18	0.0513	0.0031	6.0	0.0485
825	145	24.44	29.2	1.28	0.0425	0.0054	12.7	0.0450
835	145	24.86	30.0	1.20	0.0447	0.0026	5.8	0.0395
850	45	8.59	25.1	2.21	7.47	0.26	3.5	8.30
	60	12.77	26.7	1.90	1.68	0.12	7.1	1.75
	75	16.46	24.5	2.38	0.520	0.037	7.1	0.545
	135	24.88	26.6	1.56	0.470	0.031	6.6	0.450
	145	25.50	29.8	1.19	0.338	0.026	7.7	0.368
866	75	16.93	26.6	1.97	0.452	0.028	6.2	0.500
875	45	9.05	23.7	2.49	8.15	0.47	5.8	7.45
	60	13.42	26.4	2.05	1.34	0.058	4.3	1.57
	145	26.50	31.2	1.16	0.0315	0.0025	7.9	0.0320
900	45	9.51	25.8	2.14	5.92	0.33	5.6	6.70
	60	14.06	27.0	1.96	1.37	0.057	4.2	1.39
	75	18.02	24.8	2.36	0.470	0.017	3.6	0.429
	90	21.24	27.1	2.00	0.183	0.010	5.5	0.179
	145	27.57	27.6	1.45	0.0296	0.0020	6.7	0.0269
925	145	28.62	30.4	1.13	0.0269	0.0024	8.9	0.0246
950	145	29.68	29.3	1.26	0.0269	0.0044	16.3	0.0212
975	95	24.90	29.2	1.68	0.100	0.008	8.0	0.098
	145	30.78	30.8	1.07	0.0265	0.0033	12.4	0.0185
1000	60	16.75	24.8	2.41	0.957	0.081	8.5	0.896

[a] Refer to the definition in Sec. IV.

tions above 875 Mev show a flattening which was already noted in references 5, 6, and 7. We shall return to this matter in the subsequent discussion.

IV. PROTON FORM FACTORS

The absolute cross sections given in Table I and in Figs. 5, 6, and 7 can now be used to calculate the electromagnetic form factors of the proton as indicated in Sec. II. We show in Figs. 8 and 9 two examples in which several ellipses intersect in a common region. There are no examples among all our cases for $q^2 \leqslant 25$ which fail to give intersections. We have employed the following procedure in making the computations for the proton ellipses:

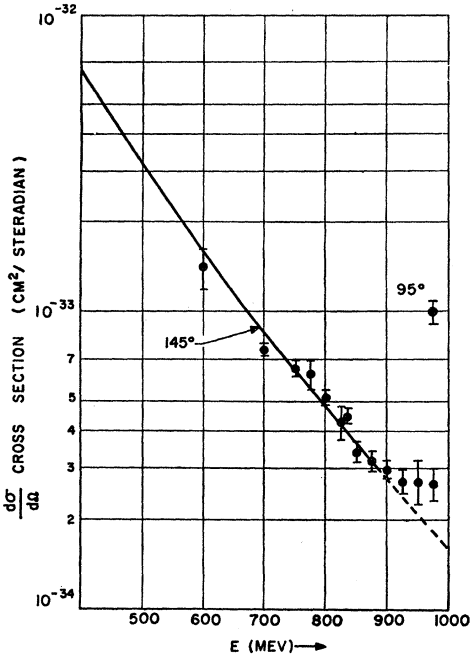

FIG. 7. This figure is similar to Fig. 5 and corresponds to the scattering angle 145°. A single point at 95° is also shown.

We have first passed smooth curves through the experimental points of Figs. 5, 6, and 7, so that at each angle we have a definite behavior of the cross sections. [In one case where we have an isolated point (975 Mev, 95°), the appropriate cross section was used with another member of a pair to find the corresponding values of F_1 and F_2.] Then we can select pairs of values (E_1,θ_1), (E_2,θ_2) from which to find intersections. As explained previously,[10,11] a small-angle cross-section ellipse intersects sharply and cleanly with an ellipse corresponding to a large-angle cross section and this type of intersection has naturally been accorded the greatest weight in our form factor analysis. When two cross sections at nearby angles are studied the intersection develops into a near-tangency and the F_1, F_2 determination can involve large errors. This behavior may be seen in Figs. 8 and 9. In Fig. 10 we illustrate the effect of experimental errors on the determination of the form factors corresponding to possible errors of $\pm 10\%$ in the cross sections. Figure 10 also shows that if the error in the cross section at the two points is in the same direction, the resulting form factor error is very small. This explains why many possible errors which are in the same direction for small and large angles have a tendency to cancel out. Such would be the case for radiative corrections.

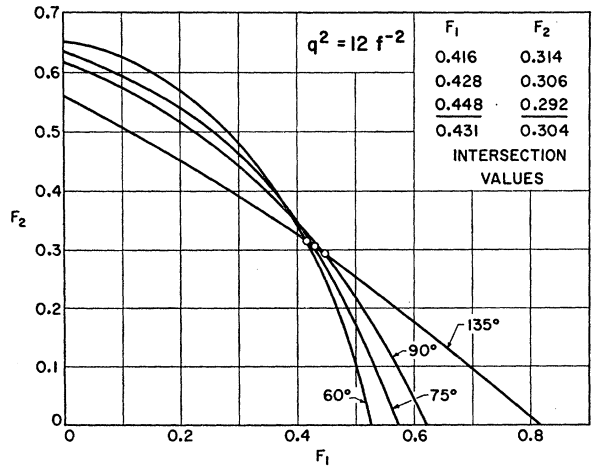

FIG. 8. This figure shows sections of elliptical arcs in the F_1, F_2 plane corresponding to the measured cross sections at the appropriate experimental conditions. The useful intersections are indicated by small circles. Note the relatively sharp intersections of small-angle and large-angle ellipses. Neighboring angles give less well determined intersections for a given experimental accuracy. "Average" intersections can be found from such plots and determine average values of F_1 and F_2. The figures for determining the averages are shown in the inset.

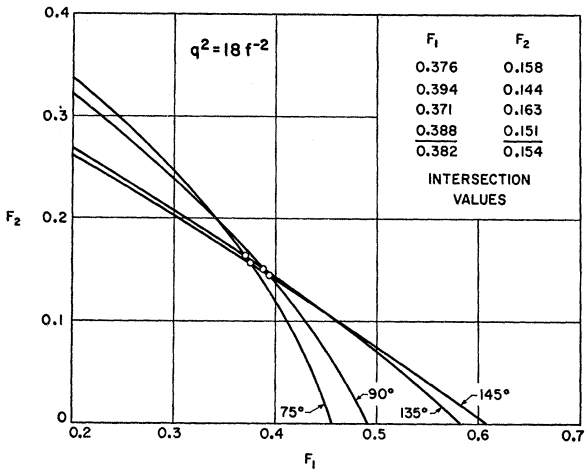

FIG. 9. This figure is similar to Fig. 8 and shows the quality of the intersections found in these experiments.

We chose eleven values of q^2 and determined at each value of q^2 the mean values of F_1 and F_2 formed by the many intersections of the corresponding ellipses. These F_1, F_2 values are then plotted, with their experimental errors, as a function of q^2, and a smooth curve can be drawn through the points. From the two form-factor curves we can then calculate a "trial" set of cross sections according to Eq. (4). By inspection we may note where the "trial" cross sections deviate most from the experiment. A little familiarity with this type of calculation immediately shows how one can get an improved fit to the data. By adjusting the F_1, F_2 vs q^2 curves a little up or down, one may obtain a second trial set of form factors and cross sections, and we may continue in the same manner. This process converges very rapidly so that within the present experimental error there is no further point in refining the fit. This second set of form factors is the set from which we calculated cross sec-

tions labeled $(d\sigma/d\Omega)_{\text{calc}}$. Table I, last column, gives this set of cross sections, which furnishes a "smoothed" set of experimental cross sections.

A "final" pair of form factor curves is shown in Fig. 11. The error bars attached to the points represent, in our best judgment, the limits of errors of the small-angle and large-angle intersections of ellipses. These limits of errors are definitely smaller than those obtainable from intersections corresponding to neighboring scattering angles. We believe that it is unrealistic, considering the present accuracy of the experiments, to give significant weight to the intersections corresponding to neighboring scattering angles.

Table II presents the numerical values of the form factors found in the above manner and shown in Fig. 11. Figure 11 and Table II are, in an important sense, the end products of this experiment.

The values of the proton form factors found from the data of this paper are in good agreement with those presented earlier[5–7] and lie within the experimental error

TABLE II. Proton form factors.[a]

q^2 in f^{-2}	F_1	$\pm\Delta F_1$	F_2	$\pm\Delta F_2$
4	0.702	0.013	0.597	0.011
6	0.602	0.009	0.487	0.009
8	0.523	0.015	0.440	0.012
10	0.491	0.019	0.343	0.013
12	0.431	0.017	0.304	0.012
14	0.396	0.017	0.261	0.011
16	0.387	0.014	0.202	0.013
18	0.382	0.012	0.154	0.010
20	0.364	0.016	0.133	0.018
22	0.350	0.006	0.100	0.008
25	0.333	0.008	0.070	0.010

[a] The errors in ΔF_1 and ΔF_2 may be approximately twice as large as given in this table, provided they are correlated. See the relevant remarks in the legend to Fig. 11.

illustrated in Fig. 1 of reference 7. In the case of the present data the curve for F_2 is apparently not about to pass through zero at $q^2=25$ f^{-2} but may do so at a larger value of q^2. In the case of F_1 the new behavior at large q^2 indicates a small but definite negative slope at $q^2\cong 25$ f^{-2} and a horizontal tangent is probably no longer likely in this region.

The question naturally arises whether these new results for $F_1(q^2)$ modify the older value of the rms radius of the electric charge distribution, which was measured as 0.80 ± 0.04 f by Hofstadter *et al.*[18] or the single determination of McAllister[19] which was 0.71 ± 0.12 f. Although we have made no special effort to measure an rms radius by concentrating on low values of q^2, an investigation of the slope of the present F_1 curve at the low values of q^2 shows that the rms radius is 0.75 ± 0.05 f, in reasonable agreement with the above values.

[18] R. Hofstadter, F. Bumiller, and M. R. Yearian, Revs. Modern Phys. **30**, 482 (1958).
[19] R. W. McAllister, thesis, Stanford University, 1960 (unpublished).

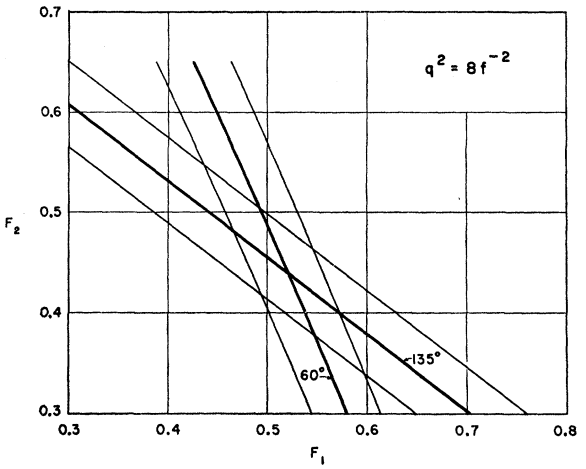

FIG. 10. This figure shows the effect of experimental errors $\pm10\%$ in the cross sections on the determinations of F_1 and F_2. Note the wide variations in the form factors if the errors have opposite signs and the smaller variations if the two errors have the same sign.

It is a remarkable fact that the experimental cross sections are very close, at all values of q^2, to the well-known "exponential" form factor behavior.[2,4,18]

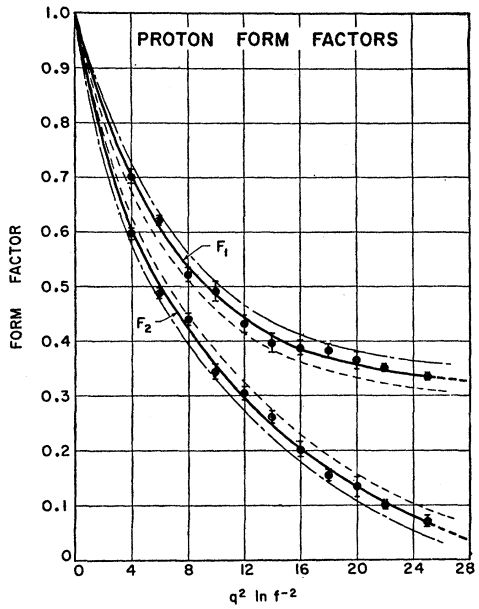

FIG. 11. This figure shows the form factors, and their errors, as found in these experiments. The corresponding values of F_1 and F_2 are also given in Table II. These same form factors have been used in the calculation of the last column of Table I. It will be noted that two dashed curves lie between the F_1, F_2 central-value solid lines. If the error limits are correlated so that they move in opposite directions, as indicated by the dashed limits, the corresponding cross sections will remain consistent with experiment. A similar statement holds for the two dot-dashed curves lying outside the F_1, F_2 central-value solid lines. Though we have not studied the correlated error question in detail we feel that the dashed and dot-dashed curves give reasonable representations of the present error limits of F_1 and F_2. Further work on errors is in progress.

The rms magnetic radius is not as well known as the electric radius, but a rough evaluation of the slope of the $F_2(q^2)$ vs q^2 curve indicates that the rms magnetic radius is 0.97 ± 0.10 f. An experiment is now in progress to try to improve the latter value.

V. INTERNAL CONSISTENCY OF THE DATA

As previously remarked, a consistent behavior of all intersections of the proton ellipses would lead to unique values of F_1 and F_2, within, of course, experimental error. Up to values of $q^2\cong25$ f^{-2}, wherever we have been able to test this question, we have observed unique values of F_1 and F_2, that is, consistency of the experiment with Rosenbluth theory. In the region between $q^2\cong25$ and 31 f^{-2}, that is, at large angles ($\cong145°$) and high energies, we do not have the ability to form intersections using higher-energy-smaller-angle data of our own, and so we cannot test the validity of the theory in this region. However, the flattening-off of the data at $\theta=145°$ between 875 and 975 Mev suggests that something strange is happening here. This flattening has been observed on several occasions. Our form-factor analysis (Table II and Fig. 11) gives the dashed behavior in the region >875 Mev in Fig. 7. We observe the rather large deviations between experiment and a continuation of "theory" in this region.

At the Washington meeting of the American Physical Society in April, 1961, we called attention to the observation that the flattening observed in these experiments at $(d\sigma/d\Omega)\cong2.7\times10^{-34}$ cm^2/sr, and in particular the point at 975 Mev and 145° ($q^2\cong30.7$ f^{-2}), is barely consistent, if not inconsistent, with a cross-section value taken from some recent measurements reported by the Cornell group[20] at 112° and ~1050 Mev between two measured points at 1000 Mev and 1100 Mev. That is, no real intersection is obtained for our 975-Mev ellipse and the Cornell ellipse. Any failure of this kind in finding consistency in the form factors would imply either: (a) some correction to the Rosenbluth formula Eq. (1) is needed, such as, e.g., one due to two-photon-virtual-exchanges, or (b) a breakdown of quantum electrodynamics, or (c) some errors in the experimental determinations. Since the flattening occurs at the extreme limits of our experimental measurements it is certainly possible that our results in this region are open to error. We do not think that this is the case because we performed various independent tests to check these results. It is to be noted that the points in the flattened region were *not* used at all in our form factor determinations. It may also still be true that the flattening represents a diffraction effect (where F_2 may go through zero) but we cannot tell that this is so at the present time. More accurate experimentation is desirable to check consistency of the proton form factors at many different values of q^2.

[20] D. N. Olson, H. F. Schopper, and R. R. Wilson, Phys. Rev. Letters **6**, 286 (1961).

VI. SIGNIFICANCE OF THE FINDINGS

Our investigation of the proton's form factors has been motivated by the desire to find a self-consistent set of values of F_1 and F_2 which gives a complete description of the behavior of an electron with the proton at the corresponding interaction vertex. For a Dirac particle of spin $\frac{1}{2}$, these two form factors are adequate to describe the interaction, as has been shown by many authors. We believe we have succeeded in our aim at least as far as $q^2\cong25$ f^{-2}. Thus the phenomenological form factors F_1, F_2 are now known in the range $0\leqslant q^2\leq25$ f^{-2} with fair accuracy. In many respects this goal has now been perhaps sufficiently well achieved at this stage of development of "fundamental" particle theory.

On the other hand, it seems likely that at least the outer parts of the electromagnetic structure of the proton are describable in terms of a more or less standard geometrical picture. Furthermore, we believe that there is definite heuristic value in having ideas about a geometrical model of a proton.

Such a model was proposed recently[9,21] in terms of a dispersion-relations suggestion for simple types of nucleon form factors associated with pion-pion interactions. Isotopic scalar and isotopic vector form factors were deduced from both experimental proton and neutron[22] form factors. The presently-determined form factors are sufficiently close to those used in the formulation of the model[9] that we have no reason, on the score of proton form factors, to alter the model or the conclusions of Hofstadter and Herman.[9]

VIII. CONCLUSIONS

(1) The splitting of the proton form factors has been confirmed.

(2) The qualitative behavior of F_1 and F_2 as functions of q^2 has been determined in the range $0\leq q^2\leq25$ f^{-2}.

(3) Good consistency in the determination of proton form factors has been found in the range $0\leq q^2\leq25$ f^{-2}. This finding serves as a support for the validity of quantum electrodynamics up to this value of q^2. Thus it is probable that quantum electrodynamics is valid at distances lying between the nucleon and pion Compton wavelengths.

(4) Some evidence for a partial breakdown in the self-consistency of the proton form factors may have been uncovered at large scattering angles (145°) at $q^2\cong30$ f^{-2}.

(5) In the range $0\leq q^2\leq25$ f^{-2} the proton form factors are in agreement with the proposed nucleon models of Hofstadter and Herman,[9] although the present results alone do not require such a model.

(6) The present results for the rms electric radius of

[21] S. Bergia, A. Stanghellini, S. Fubini, and C. Villi, Phys. Rev. Letters **6**, 367 (1961).

[22] R. Hofstadter, C. deVries, and R. Herman, Phys. Rev. Letters **6**, 290 (1961).

the proton are in reasonable agreement with the older results.[18,19]

ACKNOWLEDGMENTS

We wish to acknowledge with thanks the enthusiastic support we have had from the following members of the staff of the High-Energy Physics Laboratory: H. Dahl, G. Gilbert, C. Olson, M. Ryneveld, L. Towle, P. Wilson, and E. Wright. We are especially thankful to Mr. T. Janssens who gave us a great deal of help in using the method of intersecting ellipses. One of us (M. Croissiaux) wishes to acknowledge the kind support of Professor S. Gorodetzky and the Centre National de la Recherche Scientifique (France) in permitting him to work at Stanford University.

APPENDIX. ERRORS IN THE CROSS SECTIONS

A. The errors in part A appear in all cross sections.

(1) Incident energy in absolute units: $\pm 0.5\%$.

(2) Scattering angle, θ: $\pm 0.1°$. The errors in the cross sections vary from $\approx 1.3\%$ at $\theta = 35°$ to $\approx 0.2\%$ at $\theta = 145°$.

(3) Incident beam integration: $\pm 3\%$. The beam integration is influenced by errors in the Faraday cup, involving the measured voltage produced by the integrated charge, the value of the integration capacitor, and the automatic shutoff mechanism.

(4) Number of protons in the target: $\pm 1.5\%$. This number depends on the density of the target material, the target thickness and uniformity, and the target angle.

(5) Solid angle: $\pm 0.5\%$. Here we consider only the possible errors in the settings of the slits and their mean distances from the target. Slit openings permissible for satisfactory "optical" performance of the spectrometers have been determined experimentally.

(6) Dispersion: $\pm 1\%$.

(7) Energy calibration of the spectrometers in absolute units: $\pm 0.5\%$.

(8) Radiative corrections: $\pm 2\%$.

B. The integrated number of counts under an elastic peak is influenced by the carbon subtraction. For example, the relevant numbers for two individual cross-section curves are:

	900 Mev, 60°	900 Mev, 145°
CH_2 counts	9726	432
C counts	4370	110
H counts	5356±119	322±23

and lead to pure statistical errors of these numbers which are 2.22% and 7.14%, respectively. Most cross sections were measured more than once. In the determination of an average cross section, the error in the proton counts was used as a weight factor.

C. Although we believe that the items given in parts A and B contain all accountable errors, we found in many cases that the error in the average exceeded that predicted by pure statistical arguments. Probable sources of this behavior are instabilities in the counting electronics and in the widths of the elastic peaks under those conditions when a spectrometer field control was not available. We therefore combined the mean error of the average with the statistical errors from parts A and B and this is the error given in Table I.